On the Overlooked Structure of Stochastic Gradients

Zeke Xie[1], Qian-Yuan Tang[2], Mingming Sun[1] and Ping Li[1]

[1]Cognitive Computing Lab, Baidu Research
[2]Department of Physics, Hong Kong Baptist University
Correspondence: *xiezeke@baidu.com*,*tangqy@hkbu.edu.hk*

Abstract

Stochastic gradients closely relate to both optimization and generalization of deep neural networks (DNNs). Some works attempted to explain the success of stochastic optimization for deep learning by the arguably heavy-tail properties of gradient noise, while other works presented theoretical and empirical evidence against the heavy-tail hypothesis on gradient noise. Unfortunately, formal statistical tests for analyzing the structure and heavy tails of stochastic gradients in deep learning are still under-explored. In this paper, we mainly make two contributions. First, we conduct formal statistical tests on the distribution of stochastic gradients and gradient noise across both parameters and iterations. Our statistical tests reveal that dimension-wise gradients usually exhibit power-law heavy tails, while iteration-wise gradients and stochastic gradient noise caused by minibatch training usually do not exhibit power-law heavy tails. Second, we further discover that the covariance spectra of stochastic gradients have the power-law structures overlooked by previous studies and present its theoretical implications for training of DNNs. While previous studies believed that the anisotropic structure of stochastic gradients matters to deep learning, they did not expect the gradient covariance can have such an elegant mathematical structure. Our work challenges the existing belief and provides novel insights on the structure of stochastic gradients in deep learning.

1 Introduction

Stochastic optimization methods, such as Stochastic Gradient Descent (SGD), have been highly successful and even necessary in the training of deep neural networks (LeCun et al., 2015). It is widely believed that stochastic gradients as well as stochastic gradient noise (SGN) significantly improve both optimization and generalization of deep neural networks (DNNs) (Hochreiter and Schmidhuber, 1995, 1997; Hardt et al., 2016; Wu et al., 2021; Smith et al., 2020; Wu et al., 2020; Xie et al., 2021a; Sekhari et al., 2021; Amir et al., 2021). SGN, defined as the difference between full-batch gradient and stochastic gradient, has attracted much attention in recent years. People studied its type (Simsekli et al., 2019; Panigrahi et al., 2019; Hodgkinson and Mahoney, 2021; Li et al., 2021a), its magnitude (Mandt et al., 2017; Liu et al., 2021), its structure (Daneshmand et al., 2018; Zhu et al., 2019; Chmiel et al., 2020; Xie et al., 2021b; Wen et al., 2020), and its manipulation (Xie et al., 2021c). Among them, the noise type and the noise covariance structure are two core topics.

Topic 1. The arguments on the type and the heavy-tailed property of SGN. Recently, a line of research (Simsekli et al., 2019; Panigrahi et al., 2019; Gurbuzbalaban et al., 2021; Hodgkinson and Mahoney, 2021) argued that SGN has the heavy-tail property due to Generalized Central Limit Theorem (Gnedenko et al., 1954). Simsekli et al. (2019) presented statistical evidence showing that SGN looks closer to an α-stable distribution that has *power-law heavy tails* rather than a Gaussian distribution. (Panigrahi et al., 2019) also presented the Gaussianity tests. However, their statistical tests were actually not applied to the true SGN that is caused by minibatch sampling. Because, in this line of research, the abused notation "SGN" is studied as stochastic gradient at some iteration

37th Conference on Neural Information Processing Systems (NeurIPS 2023).

https://doi.org/10.52202/075280-2892

rather than the difference between full-batch gradient and stochastic gradient. Another line of research (Xie et al., 2021b, 2022b; Li et al., 2021a) pointed out this issue and suggested that the arguments in Simsekli et al. (2019) rely on a hidden strict assumption that SGN must be isotropic and does not hold for *parameter-dependent and anisotropic* Gaussian noise. This is why *one tail-index for all parameters* was studied in Simsekli et al. (2019). In contrast, SGN could be well approximated as an *multi-variant* Gaussian distribution in experiments at least when batch size is not too small, such as $B \geq 128$ (Xie et al., 2021b; Panigrahi et al., 2019). Another work (Li et al., 2021a) further provided theoretical evidence for supporting the anisotropic Gaussian approximation of SGN. Nevertheless, none of these works conducted statistical tests on the Gaussianity or heavy tails of the true SGN.

Contribution 1. To our knowledge, we are the first to conduct formal statistical tests on the distribution of stochastic gradients/SGN across parameters and iterations. Our statistical tests reveal that dimension-wise gradients (due to anisotropy) exhibit power-law heavy tails, while iteration-wise gradient noise (which is the true SGN due to minibatch sampling) often has Gaussian-like light tails. Our statistical tests and notations help reconcile recent conflicting arguments on Topic 1.

Topic 2. The covariance structure of stochastic gradients/SGN. A number of works (Zhu et al., 2019; Xie et al., 2021b; HaoChen et al., 2021; Liu et al., 2021; Ziyin et al., 2022) demonstrated that the anisotropic structure and sharpness-dependent magnitude of SGN can help escape sharp minima efficiently. Moreover, some works theoretically demonstrated (Jastrzkebski et al., 2017; Zhu et al., 2019) and empirically verified (Xie et al., 2021b, 2022b; Daneshmand et al., 2018) that the covariance of SGN is approximately equivalent to the Hessian near minima. However, this approximation is only applied to minima and along flat directions corresponding to nearly-zero Hessian eigenvalues. The quantitative structure of stochastic gradients itself is still largely overlooked by previous studies.

Contribution 2. We surprisingly discover that the covariance of stochastic gradients has the power-law spectra in deep learning, which is overlooked by previous studies. While previous studies believed that the anisotropic structure of stochastic gradients matters to deep learning, they did not expect the gradient covariance can have such an elegant power-law structure. The power-law gradient covariance may help understand the success of stochastic optimization for deep learning.

2 Preliminaries

Notations. Suppose a neural network f_θ has n model parameters as θ. We denote the training dataset as $\{(x, y)\} = \{(x_j, y_j)\}_{j=1}^N$ drawn from the data distribution $\mathcal{S}$ and the loss function over one data sample $\{(x_j, y_j)\}$ as $l(\theta, (x_j, y_j))$. We denote the training loss as $L(\theta) = \frac{1}{N}\sum_{j=1}^N l(\theta, (x_j, y_j))$.

We compute the gradients of the training loss with the batch size B and the learning rate η for T iterations. We let $g^{(t)}$ represent the stochastic gradient at the t-th iteration. We denote the *Gradient History Matrix* as $G = [g^{(1)}, g^{(2)}, \cdots, g^{(T)}]$ an $n \times T$ matrix where the column vector $G_{:,t}$ represents the *dimension-wise gradients* $g^{(t)}$ for n model parameters, the row vector $G_{i,:}$ represents the *iteration-wise gradients* $g_i^{:}$ for T iterations, and the element $G_{i,t}$ is $g_i^{(t)}$ at the t-th iteration for the parameter θ_i. We analyze G for a given model without updating the model parameter θ. The Gradient History Matrix G plays a key role in reconciling the conflicting arguments on Topic 1. Because the defined dimension-wise SGN (due to anisotropy) is the abused "SGN" in one line of research (Simsekli et al., 2019; Panigrahi et al., 2019; Gurbuzbalaban et al., 2021; Hodgkinson and Mahoney, 2021), while iteration-wise SGN (due to minibatch sampling) is the true SGN as another line of research (Xie et al., 2021b, 2022b; Li et al., 2021a) suggested. Our notation mitigates the abused "SGN".

We further denote the second moment as $C_m = \mathbb{E}[gg^\top]$ for stochastic gradients and the covariance as $C = \mathbb{E}[(g - \bar{g})(g - \bar{g})^\top]$ for SGN, where $\bar{g} = \mathbb{E}[g]$ is the full-batch gradient. We denote the descending ordered eigenvalues of a matrix, such as the Hessian H and the covariance C, as $\{\lambda_1, \lambda_2, \ldots, \lambda_n\}$ and denote the corresponding spectral density function as $p(\lambda)$.

Goodness-of-Fit Test. In statistics, various Goodness-of-Fit Tests have been proposed for measuring the goodness of empirical data fitting to some distribution. In this subsection, we introduce how to conduct the Kolmogorov-Smirnov (KS) Test (Massey Jr, 1951; Goldstein et al., 2004) for measuring the goodness of fitting a power-law distribution and the Pearson's χ^2 Test (Plackett, 1983) for measuring the goodness of fitting a Gaussian distribution. We present more details in Appendix B.

https://doi.org/10.52202/075280-2892

Table 1: The KS and χ^2 statistics and the hypothesis acceptance rates of the gradients over dimensions and iterations, respectively. Model: LeNet. Batch Size: 100. In the second column "random" means randomly initialized models, while "pretrain" means pretrained models.

Dataset	Training	SG Type	$\bar{d}_{\text{ks}}$	d_c	Power-Law Rate	$\bar{p}$-value	Gaussian Rate
MNIST	Random	Dimension	0.0355	0.0430	76.6%	4.11×10^{-4}	0.18%
MNIST	Random	Iteration	0.191	0.0430	0.0788%	0.321	65.1%
MNIST	Pretrain	Dimension	0.0401	0.0430	60.6%	5.77×10^{-4}	0.24%
MNIST	Pretrain	Iteration	0.179	0.0430	0.052%	0.306	62.0%
CIFAR-10	Random	Dimension	0.0330	0.0430	81.8%	1.03×10^{-3}	0.3%
CIFAR-10	Random	Iteration	0.574	0.0430	0%	0.337	66.8%
CIFAR-10	Pretrain	Dimension	0.0381	0.0430	69.2%	4.01×10^{-5}	0%
CIFAR-10	Pretrain	Iteration	0.654	0.0430	0%	0.275	56.6%

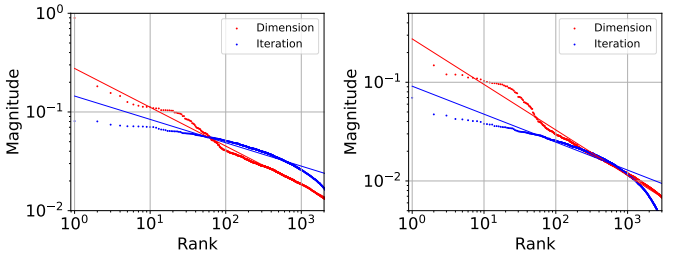

Figure 1: Magnitude of gradients w.r.t. magnitude rank. The dimension-wise gradients (one column vector of G) have power-law heavy tails, while the iteration-wise gradients (one row vector of G) have no power-law heavy tails. Model: (Randomly Initialized) LeNet. Dataset: MNIST and CIFAR-10.

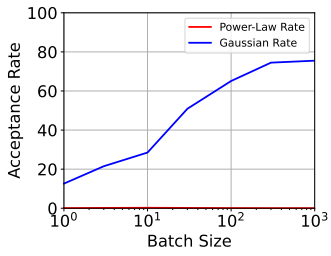

Figure 2: The power-law rates and Gaussian rates w.r.t. batch size. Increasing batch size significantly improves the Gaussianity of SGN. Model: LeNet.

When we say a set of random variables (the elements or eigenvalues) is approximately power-law/Gaussian in this paper, we mean the tested set of data points can pass KS Tests for power-law distributions or χ^2 Test for Gaussian distributions at the Significance Level 0.05. We note that, in all statistical tests of this paper, we set the Significance Level as 0.05.

In KS Test, we state *the power-law hypothesis* that the tested set of elements is power-law. If the KS distance d_{ks} is larger than the critical distance d_c, the KS test will reject the power-law hypothesis. In contrast, if the KS distance d_{ks} is less than the critical distance d_c, the KS test will support (not reject) the power-law hypothesis. The smaller d_{ks} is, the better the goodness-of-power-law is.

In χ^2 Test, we state *the Gaussian hypothesis* that the tested set of elements is Gaussian. If the estimated p-value is larger than 0.05, the χ^2 test will reject the Gaussian hypothesis. If the estimated p-value is less than 0.05, the χ^2 test will support (not reject) the Gaussian hypothesis. The smaller p-value is, the better the goodness-of-Gaussianity is.

The Gaussianity test consists of Skewness Test and Kurtosis Test (Cain et al., 2017) (Pleas see Appendix B) for more details. Skewness is a measure of symmetry. A distribution or dataset is symmetric if the distribution on either side of the mean is roughly the mirror image of the other. Kurtosis is a measure of whether the data are heavy-tailed or light-tailed relative to a normal distribution. Empirical data with high (respectively, low) kurtosis tend to have heavy (respectively, light) tails. Thus, χ^2 Test can reflect both Gaussianity and heavy tails.

3 Rethink Heavy Tails in Stochastic Gradients

In this section, we try to reconcile the conflicting arguments on Topic 1 by formal statistical tests.

The power-law distribution. Suppose that we have the set of k random variables $\{\lambda_1, \lambda_2, \ldots, \lambda_k\}$ that obeys a power-law distribution. We may write the probability density function of a power-law distribution as

$$p(\lambda) = Z^{-1}\lambda^{-\beta}, \tag{1}$$

66259 https://doi.org/10.52202/075280-2892

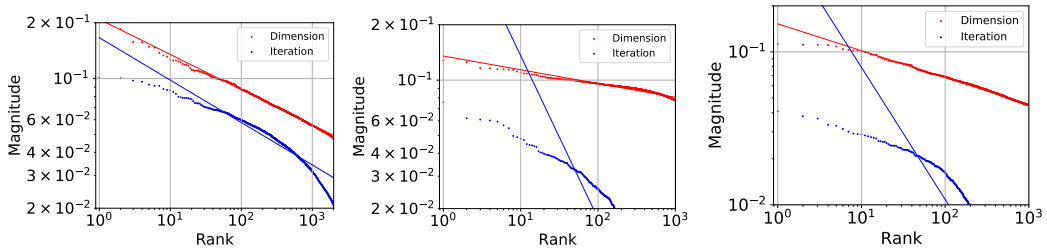

(a) Random FCN on MNIST (b) Random ResNet18 on CIFAR-10 (c) Random ResNet18 on CIFAR-100

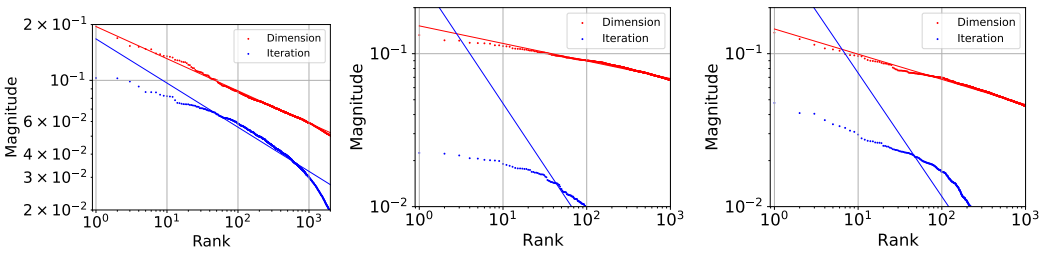

(d) Pretrained FCN on MNIST (e) Pretrained ResNet18 on CIFAR-10 (f) Pretrained ResNet18 on CIFAR-100

Figure 3: We plot the magnitude of gradients with respect to the magnitude rank for FCN and ResNet18 on MNIST, CIFAR-10, and CIFAR-100. The dimension-wise gradients have power-law heavy tails, while the iteration-wise gradients have no power-law heavy tails.

where Z is the normalization factor. The finite-sample power law, also known as Zipf's law, can also be approximately written as

$$\lambda_k = \lambda_1 k^{-s}, \tag{2}$$

if we let $s = \frac{1}{\beta - 1}$ denote the power exponent of Zipf's law (Visser, 2013). A well-known property of power laws is that, when the power-law variables and their corresponding rank orders are scattered in log-log scaled plot, a straight line may fit the points well (Clauset et al., 2009).

Dimension-wise gradients are usually power-law, while iteration-wise gradients are usually Gaussian. In Figure 1, we plot dimension-wise gradients and iteration-wise gradients of LeNet on MNIST and CIFAR over 5000 iterations with fixing the model parameters. We leave experimental details in Appendix A and the extensive statistical test results in Appendix C. In Figure 1, while some points slightly deviate from the fitted straight line, we may easily observe the straight lines approximately fit the red points (dimension-wise gradients) but fail to fit the blue points (iteration-wise gradients). The observations indicate that dimension-wise gradients have power-law heavy tails while iteration-wise gradients have no such heavy tails.

Table 1 shows the mean KS distance and the mean p-value over dimensions and iterations as well as the power-law rates and the Gaussian rates. We note that the power-law/Gaussian rate means the percentage of the tested points that are not rejected for the power-law/Gaussian hypothesis via KS/χ^2 tests. Dimension-wise gradients and iteration-wise gradients show significantly different preferences for the power-law rate and the Gaussian rate. For example, a LeNet on CIFAR-10 has 62006 model parameters. Dimension-wise gradients of the model are power-law for 81.8% iterations and are Gaussian for only 0.3% iterations. In contrast, iteration-wise gradients of the model are Gaussian for 66.8% dimensions (parameters) and are power-law for no dimension.

The observation and the statistical test results of Table 1 both indicate that dimension-wise gradients usually have power-law heavy tails while iteration-wise gradients are usually approximately Gaussian (with light tails) for most dimensions. The conclusion holds for both pretrained models and random models on various datasets. Similarly, we also observe power-law dimension-wise gradients and non-power-law iteration-wise gradients for FCN and ResNet18 in Figure 3, as well as Table 5 in Appendix C.

https://doi.org/10.52202/075280-2892

According to Central Limit Theorem, the Gaussianity of iteration-wise gradients should depend on the batch size. We empirically studied how the Gaussian rate of iteration-wise gradients depends on the batch size. The results in Figure 2 and Table 4 (see Appendix) support that the Gaussianity of iteration-wise gradients indeed positively correlates to the batch size, which is consistent with the Central Limit Theorem. In the common setting that $B \geq 30$, the Gaussianity of SGN can be statistically more significant than heavy tails for most parameters of DNNs, according to χ^2 Tests.

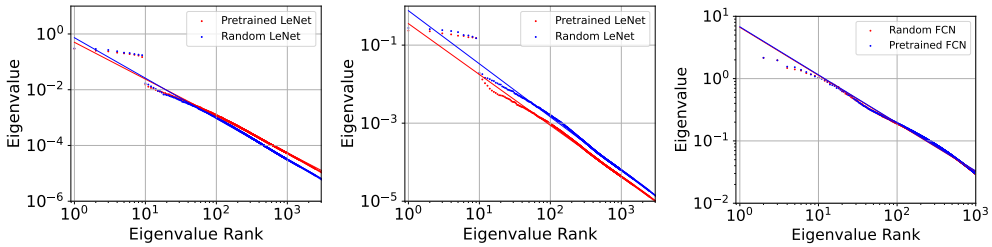

(a) MNIST (b) CIFAR-10 (c) MNIST

Figure 4: The gradient spectra are highly similar and exhibit power laws for both random models and pretrained models. Model: LeNet and 2-Layer FCN. Dataset: MNIST and CIFAR-10.

Reconciling the conflicting arguments on Topic 1. We argue that the power-law tails of dimension-wise gradients and the Gaussianity of iteration-wise gradients may well explain the conflicting arguments on Topic 1. On the one hand, the evidences proposed by the first line of research are mainly for describing the elements of one column vector of G which represent the dimension-wise gradient at a given iteration. Thus, the works in the first line of research can only support that the distribution of (dimension-wise) stochastic gradients has a power-law heavy tail, where heavy tails are mainly caused by the gradient covariance (See Section 4) instead of minibatch training.

On the other hand, the works in the second line of research pointed out that the type of SGN is actually decided by the distribution of (iteration-wise) stochastic gradients due to minibatch sampling, which is usually Gaussian for a common batch size $B \geq 30$. Researchers care more about the true SGN, the difference between full-batch gradients and stochastic gradients, mainly because SGN essentially matters to implicit regularization of SGD and deep learning dynamics (Jastrzkebski et al., 2017; Zhu et al., 2019; Xie et al., 2021b; Li et al., 2021b). While previous works in the second line of research did not conduct statistical tests, our work fills the gap.

In summary, while it seems that the two lines of research have conflicting arguments on Topic 1, their evidences are actually not contradicted. We may easily reconcile the conflicts as long as the first line of research clarifies that the heavy-tail property describes dimension-wise gradients (not SGN), which corresponds to the column vector of G instead of the row vector of G.

We notice that the Gaussian rates (the rates of not rejecting the Gaussian hypothesis) do not approach to a very high level (e.g. 95%) even under relatively large batch sizes (e.g., $B = 1000$), while they have nearly zero power-law rates (the rates of not rejecting the power-law hypothesis). While the Gaussian rate is low under small batch sizes, the power-law rate is still nearly zero. This may indicate that SGN of a small number of model parameters or under small batch sizes may have novel properties beyond the Gaussianity and the power-law heavy tails that previous works expected.

4 The Overlooked Power-Law Structure

In this section, we study the covariance/second-moment structure of stochastic gradients. Despite the reconciled conflicts on Topic 1, another question arises that why dimension-wise stochastic gradients may exhibit power laws in deep learning. We show that the covariance not only explains why power-law gradients arise but also surprisingly challenges conventional knowledge on the relation between the covariance (of SGN) and the Hessian (of the training loss).

The power-law covariance spectrum. We display the covariance spectra for various models on MNIST and CIFAR-10. Figure 4 shows the covariance spectra for pretrained models and random models are both power-law despite several slightly deviated top eigenvalues. The KS test results are shown in Table 2. To our knowledge, we are the first to discover that the covariance spectra are usually power-law for deep learning with formal empirical & statistical evidences.

https://doi.org/10.52202/075280-2892

Table 2: KS statistics of the covariance spectra of LeNet and FCN.

Dataset	Model	Training	d_{ks}	d_{c}	Power-Law	$\hat{s}$
MNIST	LeNet	Pretrain	0.0206	0.043	Yes	1.302
MNIST	LeNet	Random	0.0220	0.043	Yes	1.428
CIFAR-10	LeNet	Pretrain	0.0201	0.043	Yes	1.257
CIFAR-10	LeNet	Random	0.0214	0.043	Yes	1.300
MNIST	FCN	Pretrain	0.0415	0.043	Yes	0.866
MNIST	FCN	Random	0.0418	0.043	Yes	0.864

The relation between gradient covariances and Hessians. Both SGN and Hessian essentially matter to optimization and generalization of deep learning (Li et al., 2020; Ghorbani et al., 2019; Zhao et al., 2019; Jacot et al., 2019; Yao et al., 2018; Dauphin et al., 2014; Byrd et al., 2011). A conventional belief is that the covariance is approximately proportional to the Hessian near minima, namely $C(\theta) \propto H(\theta)$ (Jastrzkebski et al., 2017; Zhu et al., 2019; Xie et al., 2021b, 2022b; Daneshmand et al., 2018; Liu et al., 2021). Near a critical point, we have

$$C(\theta) \approx \frac{1}{B}\left[\frac{1}{N}\sum_{j=1}^{N}\nabla l(\theta,(x_j,y_j))\nabla l(\theta,(x_j,y_j))^{\top}\right]\frac{1}{B}\text{FIM}(\theta) \approx \frac{1}{B}[H(\theta)], \tag{3}$$

where $\text{FIM}(\theta)$ is the observed Fisher Information matrix, referring to Chapter 8 of Pawitan (2001) and Zhu et al. (2019). The first approximation holds when the expected gradient is small near minima, and the second approximation hold because FIM is approximately equal to the Hessian near minima.

Some works (Xie et al., 2021b, 2022b) empirically verified Eq. (3) and further argued that Eq. (3) approximately holds even for random models (which are far from minima) in terms of the flat directions corresponding to small eigenvalues of the Hessian. Note that the most eigenvalues of the Hessian are nearly zero. The gradients along these flat directions are nearly zero as the approximation in Eq. (3) is particularly mild along these directions.

The common PCA method, as well as the related low-rank matrix approximation, actually prefers to remove or ignore the components corresponding to small eigenvalues. Because the top eigenvalues and their corresponding eigenvectors can reflect the main properties of a matrix. Unfortunately, previous works (Xie et al., 2021b, 2022b) only empirically studied the small eigenvalues of the covariance and the Hessian and missed the most important top eigenvalues. The missing evidence for verifying the top eigenvalues of the covariance and the Hessian can be a serious flaw for the well-known approximation Eq. (3). A number of works (Sagun et al., 2016, 2017; Wu et al., 2017; Pennington and Bahri, 2017; Pennington and Worah, 2018; Papyan, 2018, 2019; Jacot et al., 2019; Fort and Scherlis, 2019; Singh et al., 2021; Liao and Mahoney, 2021; Xie et al., 2022a) tried to analyze the Hessian structure of deep loss landscape. However, they did not formally touch the structure of stochastic gradients. In this paper, we particularly compute the top thousands of eigenvalues of the Hessian and compare them to the corresponding top eigenvalues of the covariance.

In Figure 5, we discover that, surprisingly, the top eigenvalues of the covariance can significantly deviate from the corresponding eigenvalues of the Hessian sometimes by more than one order of magnitude near or far from minima. This challenges the conventional belief on the proportional relation between the covariance and the Hessian near minima.

We also note that the covariance and the second-moment matrix have highly similar spectra in the log-scale plots. For simplicity of expressions, when we say the spectra of gradient noise/gradients in the following analysis, we mean the spectra of the covariance/the second moment, respectively.

For pretrained models, especially pretrained FCN, while the magnitudes of the Hessian and the corresponding covariance are not even close, the straight lines fit the Hessian spectra and the covariance spectra well. Moreover, the fitted straight lines have similar slopes. Our results also support a very recent finding (Xie et al., 2022a) that the Hessians have power-law spectra for well-trained DNNs but significantly deviate from power laws for random DNNs.

For random models, while the Hessian spectra are not power-law, the covariance spectra surprisingly still exhibit power-law distributions. This is beyond the existing work expected. It is not surprising that the Hessian and the covariance have no close relation without pretraining. However, we report

https://doi.org/10.52202/075280-2892

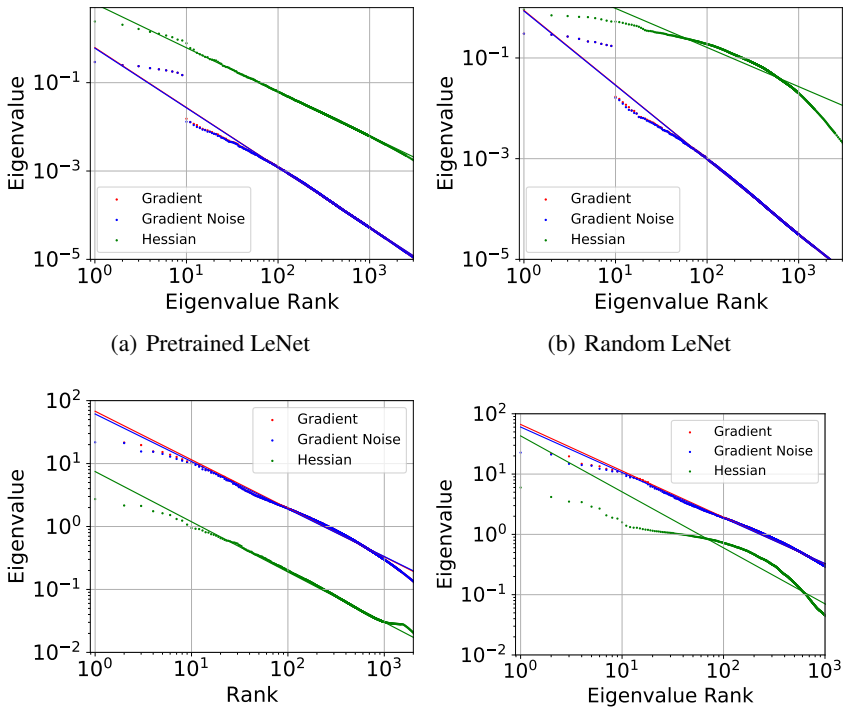

(a) Pretrained LeNet (b) Random LeNet

(c) Pretrained FCN (d) Random FCN

Figure 5: The spectra of gradients (Uncentered Covariance), gradient noise (Centered Covariance), and Hessians for random models and pretrained models. Model: LeNet and FCN. Dataset: MNIST.

that the power-law covariance spectrum seems to be a universal property, and it is more general than the power-law Hessian spectrum for DNNs.

Robust and low-dimensional learning subspace. May power-law covariance spectra theoretically imply any novel insight? The answer is affirmative. A number of papers (Gur-Ari et al., 2018; Ghorbani et al., 2019; Xie et al., 2021b) reported that deep learning (via SGD) mainly happens in a low-dimensional space spanned by the eigenvectors corresponding to large eigenvalues during the whole training process. Note that the low-dimensional learning space implicitly reduces deep models' complexity. These studies indicated that the intrinsic dimension of learning space is much lower than the original model dimensionality, resulting in improved generalization and low complexity of deep models. However, existing work cannot explain why the learning space is low-dimensional and robust during training. In this paper, robust space means that the space's dimensions are stable during training. We argue that the power-law structure can mathematically explain why low-dimensional and robust learning space exists.

We try to mathematically answer this question by studying the gradient covariance eigengaps. We define the k-th eigengap as $\delta_k = \lambda_k - \lambda_{k+1}$. According to Eq. (2), we have δ_k approximately meeting

$$\delta_k = \mathrm{Tr}(C) Z_d^{-1} (k^{-\frac{1}{\beta-1}} - (k+1)^{-\frac{1}{\beta-1}}) = \lambda_k \left[1 - (\frac{k}{k+1})^s \right], \tag{4}$$

where $Z_d = \sum_{k=1}^{n} k^{-\frac{1}{\beta-1}}$ is the normalization factor. Interestingly, it demonstrates that eigengaps also approximately exhibit a power-law distribution. We present the empirical evidences of the power-law eigengaps in Figure 16 and Table 3 (of Appendix C). We observe that the eigengaps decay faster than the eigenvalue. This is not surprising. For example, under the approximation $s \approx 1$, we have an approximate power-law decaying

$$\delta_k = \mathrm{Tr}(C) Z_d^{-1} (k+1)^{-(s+1)} \tag{5}$$

with a larger power exponent as $s+1$.

Based on the Davis-Kahan $\sin(\Theta)$ Theorem (Davis and Kahan, 1970), we use the angle of the original eigenvector u_k and the perturbed eigenvector $\tilde{u}_k$, namely $\langle u_k, \tilde{u}_k \rangle$, to measure the robustness of

https://doi.org/10.52202/075280-2892

space's dimensions. We apply Theorem 1, a useful variant of Davis-Kahan Theorem (Yu et al., 2015), to the gradient covariance in deep learning, which states that the eigenspace (spanned by eigenvectors) robustness can be well bounded by the corresponding eigengap.

Theorem 1 (Eigengaps Bound Eigenspace Robustness (Yu et al., 2015))**.** *Suppose the true gradient covariance is C, the perturbed gradient covariance is $\tilde{C} = C + \epsilon M$, the i-th eigenvector of C is u_i , and its corresponding perturbed eigenvector is $\tilde{u}_i$. Under the conditions of the Davis-Kahan Theorem, we have*

$$\sin\langle u_k, \tilde{u}_k\rangle \leq \frac{2\epsilon\|M\|_{op}}{\min(\lambda_{k-1} - \lambda_k, \lambda_k - \lambda_{k+1})},$$

where $\|M\|_{op}$ is the operator norm of M.

As we have a small number of large eigengaps corresponding to the large eigenvalues, the corresponding learning space robustness has a tight upper bound. For example, given the power-law eigengaps in Eq. (5), the upper bound of eigenvector robustness can be approximately written as

$$\sup \sin\langle u_k, \tilde{u}_k\rangle \approx \frac{2\epsilon\|M\|_{op}(k+1)^{s+1}}{\lambda_1}, \tag{6}$$

when s is close to one. Obviously, the bound is relatively tight for top dimensions (small k) but becomes very loose for tailed dimensions (large k). A similar conclusion also holds given Eq. (4) without $s \approx 1$. This indicates that non-top eigenspace can be highly unstable during training, because δ_k can decay to nearly zero for a large k. To the best of our knowledge, we are the first to demonstrate that the robustness of low-dimensional learning space directly depends on the eigengaps.

Note that the existence of top large eigenvalues does not necessarily indicate their gaps are also statistically large. Previous papers failed to reveal that top eigengaps also dominate tailed eigengaps in deep learning. Fortunately, we numerically demonstrate that, as rank order increases, both eigenvalues and eigengaps decay. Eigengaps even decay faster than eigenvalues due to the larger magnitude of the power exponent. Our analysis partially explains the foundation of learning space robustness in deep learning.

5 Empirical Analysis and Discussion

In this section, we empirically studied the covariance spectrum for DNNs in extensive experiments. We particularly reveal that when the power-law covariance for DNNs appears or disappears. We leave experimental details in Appendix A

1. Batch Size. Figure 6 shows that the power-law covariance exists in deep learning for various batch sizes. Moreover, the top eigenvalues are indeed approximately inverse to the batch size as Eq. (3) suggests, while the proportional relation between the Hessian and the covariance is weak.

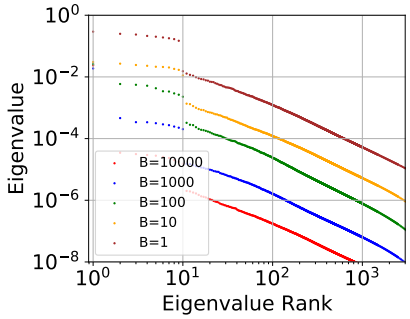

Figure 6: Power-law covariance is approximately inverse to the batch size in deep learning. Model: LeNet. Dataset: MNIST.

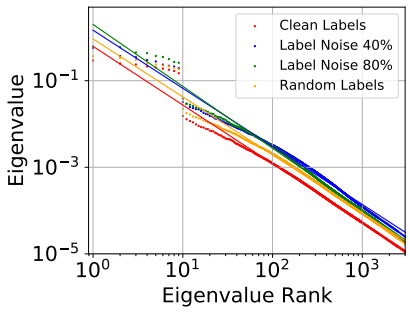

Figure 7: Comparison of the gradient spectra on MNIST with clean labels, noisy labels, and random labels. Model: LeNet.

2. Learning with Noisy Labels and Random Labels. Recently, people usually regarded learning with noisy labels (Han et al., 2020) as an important setting for exploring the overfitting and generalization of DNNs. Previous papers (Martin and Mahoney, 2017; Han et al., 2018) demonstrated that DNNs may easily overfit noisy labels and even have completely random labels during training, while

https://doi.org/10.52202/075280-2892

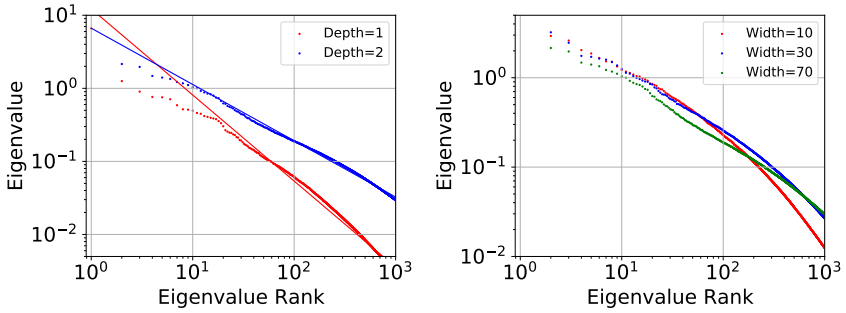

Figure 8: Large enough width (e.g., Width$\geq$ 70) matters to the goodness of power-law covariance, while the depth does not. Left: FCN with various depths. Right: FCN with various widths.

convergence speed is slower compared with learning with clean labels. Is this caused by the structure of stochastic gradients? It seems no. We compared the covariance spectrum under clean labels, 40% noisy labels, 80% noisy labels, and completely random labels in Figure 7. We surprisingly discovered that memorization of noisy labels matters little to the power-law structure of stochastic gradients.

3. Depth and Width. In this paper, we also study how the depth and the width of neural networks affect the power-law covariance. Figure 8 and the KS tests in Table 8 (Appendix C) support that certain width (e.g., Width$\geq$ 70) is often required for supporting the power-law hypothesis, while the depth seems unnecessary. Even one-layer FCN may still exhibit the power-law covariance.

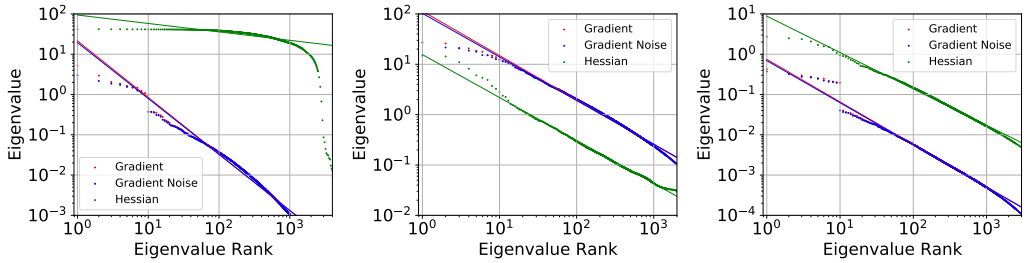

(a) LNN (b) LNN+BatchNorm (c) LNN+ReLU

Figure 9: The power-law gradients appear in LNNs with BatchNorm or ReLU, but disappear in fully LNNs. Dataset: MNIST.

4. Linear Neural Networks (LNNs) and Nonlinearity. What is the simplest model that shows the power-law covariance? We study covariance spectra for fully LNNs, LNNs with BatchNorm, and LNNs with ReLU (FCN w/o BatchNorm) in Figure 9. Obviously, fully LNNs may not learn minima with power-law Hessians. Layer-wise nonlinearity seems necessary for the power-law Hessian spectra (Xie et al., 2022a). However, even the simplest two-layer LNN with no nonlinearity still exhibits power-law covariance.

5. The Outliers, BatchNorm, and Data Classes. We also report that there sometimes exist a few top covariance eigenvalues that significantly deviate from power laws or the fitted straight lines. Figure 11 shows that, the outliers are especially significant for LeNet, a Convolution Neural Network, but less significant for FCN. We also note that LeNet does not apply BatchNorm, while the used FCN applies BatchNorm. What is the real factor that determines whether top outliers are significant or not? Figures 9 and 10 support that it is BatchNorm that makes top outliers less significant rather than the convolution layers. Because even the simplest LNNs, which have no convolution layers and nonlinear activations, still exhibit significant top outliers. This may explain why BatchNorm helps training of DNNs.

Suppose there are c classes in the dataset, where $c = 10$ for CIFAR-10 and MNIST. We observe that the number of outliers is usually $c - 1$ in Figures 11 and 12. It supports that the gradients of DNNs indeed usually concentrate in a tiny top space as previous work suggested (Gur-Ari et al., 2018), because the ninth eigenvalue may be larger than the tenth eigenvalue by one order of magnitude. However, this conclusion may not hold similarly well without BatchNorm.

66265 https://doi.org/10.52202/075280-2892

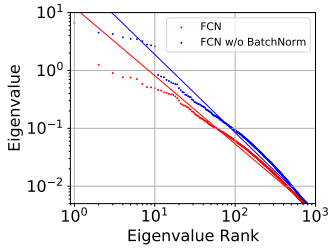

Figure 10: BatchNorm can make the outliers less significant. Model: FCN with/without BatchNorm.

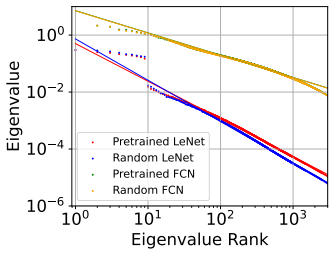

Figure 11: The number of outliers is usually $c-1$. The outliers of the FCN gradient spectrum is much less significant than that of LeNet. Dataset: MNIST.

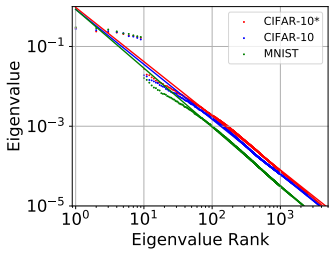

Figure 12: The outliers in the power-law spectrum mainly depends on the the number of data classes rather than the number of model outputs (logits).

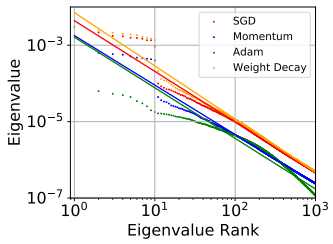

Figure 13: Momentum and Weight Decay does not significantly affect the power-law covariance, while Adam does.

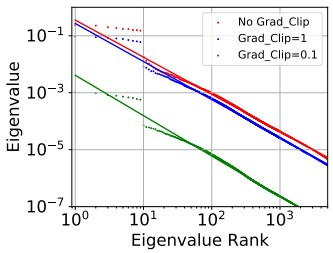

Figure 14: The power-law covariance holds with Gradient Clipping. Model: LeNet. Dataset: CIFAR-10.

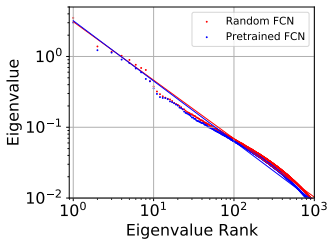

Figure 15: The power-law gradients appear on non-image natural datasets. Dataset: Avila. Model: FCN.

Is it possible that the number of outliers depends on the number of model outputs (logits) rather than the number of data classes? In Figure 12, we eliminate the possibility by training a LeNet with 100 logits on CIFAR-10, denoted by CIFAR-10*. The number of outliers will be constant even if we increase the model logits.

6. Optimization Techniques. Previous papers report that Weight Decay, Momentum, and Adam may significantly affect gradient noise (Sutskever et al., 2013; Daneshmand et al., 2018; Xie et al., 2023). In Figure 13, we discover that Weight Decay and Momentum do not affect the power-law structure, while Adam obviously breaks the power-law structure due to adaptive gradients. Gradient Clipping is a popular method for stabilizing and accelerating the training of language models (Zhang et al., 2019). Figure 14 shows Gradient Clipping does not break the power-law structure.

7. Non-image Data. Natural images have special statistical properties (Torralba and Oliva, 2003). May the power-law covariance be caused by the statistical properties of natural images? In Figure 15 on a non-image UCI dataset, Avila, which is a simple classification dataset with only ten input features, the power-law gradients of DNNs are more general than natural image statistics.

6 Conclusion

In this paper, we revisit two essentially important topics about stochastic gradients in deep learning. First, we reconciled recent conflicting arguments on the heavy-tail properties of SGN. We demonstrated that dimension-wise gradients usually have power-law heavy tails, while iteration-wise gradients or SGN have relatively high Gaussianity. Second, to our knowledge, we are the first to report that the covariance of gradients usually has a surprising power-law structure in even simple neural networks. The heavy tails of dimension-wise gradients could be explained as a natural result of the power-law covariance. We further analyze the theoretical implications and how various settings affect the power-law gradient structure in deep learning. The main limitations of our work lie in lacking (1) theoretically explaining why the power-law covariance generally exists in deep learning and (2) scaling the experiments to larger Transformer-based models. We leave the theoretical explanation and the results of large Transformer-based models as future work.

https://doi.org/10.52202/075280-2892

Acknowledgement

We thank Ms. Zheng He for reproducing core experimental results. This work is supported by the Early Career Scheme (ECS) from the Research Grants Council (RGC) of Hong Kong (No. 22302723).

References

Alstott, J., Bullmore, E., and Plenz, D. (2014). powerlaw: a python package for analysis of heavy-tailed distributions. *PloS one*, 9(1):e85777.

Amir, I., Koren, T., and Livni, R. (2021). Sgd generalizes better than gd (and regularization doesn't help). In *Conference on Learning Theory*, pages 63–92. PMLR.

Byrd, R. H., Chin, G. M., Neveitt, W., and Nocedal, J. (2011). On the use of stochastic hessian information in optimization methods for machine learning. *SIAM Journal on Optimization*, 21(3):977–995.

Cain, M. K., Zhang, Z., and Yuan, K.-H. (2017). Univariate and multivariate skewness and kurtosis for measuring nonnormality: Prevalence, influence and estimation. *Behavior research methods*, 49(5):1716–1735.

Chmiel, B., Ben-Uri, L., Shkolnik, M., Hoffer, E., Banner, R., and Soudry, D. (2020). Neural gradients are near-lognormal: improved quantized and sparse training. In *International Conference on Learning Representations*.

Clauset, A., Shalizi, C. R., and Newman, M. E. (2009). Power-law distributions in empirical data. *SIAM review*, 51(4):661–703.

Daneshmand, H., Kohler, J., Lucchi, A., and Hofmann, T. (2018). Escaping saddles with stochastic gradients. In *International Conference on Machine Learning*, pages 1155–1164.

Dauphin, Y. N., Pascanu, R., Gulcehre, C., Cho, K., Ganguli, S., and Bengio, Y. (2014). Identifying and attacking the saddle point problem in high-dimensional non-convex optimization. *Advances in Neural Information Processing Systems*, 27:2933–2941.

Davis, C. and Kahan, W. M. (1970). The rotation of eigenvectors by a perturbation. iii. *SIAM Journal on Numerical Analysis*, 7(1):1–46.

De Stefano, C., Maniaci, M., Fontanella, F., and di Freca, A. S. (2018). Reliable writer identification in medieval manuscripts through page layout features: The "avila" bible case. *Engineering Applications of Artificial Intelligence*, 72:99–110.

Fort, S. and Scherlis, A. (2019). The goldilocks zone: Towards better understanding of neural network loss landscapes. In *Proceedings of the AAAI Conference on Artificial Intelligence*, volume 33, pages 3574–3581.

Ghorbani, B., Krishnan, S., and Xiao, Y. (2019). An investigation into neural net optimization via hessian eigenvalue density. In *International Conference on Machine Learning*, pages 2232–2241. PMLR.

Gnedenko, B., Kolmogorov, A., Gnedenko, B., and Kolmogorov, A. (1954). Limit distributions for sums of independent. *Am. J. Math*, 105.

Goldstein, M. L., Morris, S. A., and Yen, G. G. (2004). Problems with fitting to the power-law distribution. *The European Physical Journal B-Condensed Matter and Complex Systems*, 41(2):255–258.

Gur-Ari, G., Roberts, D. A., and Dyer, E. (2018). Gradient descent happens in a tiny subspace. *arXiv preprint arXiv:1812.04754*.

Gurbuzbalaban, M., Simsekli, U., and Zhu, L. (2021). The heavy-tail phenomenon in sgd. In *International Conference on Machine Learning*, pages 3964–3975. PMLR.

https://doi.org/10.52202/075280-2892

Han, B., Yao, Q., Liu, T., Niu, G., Tsang, I. W., Kwok, J. T., and Sugiyama, M. (2020). A survey of label-noise representation learning: Past, present and future. *arXiv preprint arXiv:2011.04406*.

Han, B., Yao, Q., Yu, X., Niu, G., Xu, M., Hu, W., Tsang, I., and Sugiyama, M. (2018). Co-teaching: Robust training of deep neural networks with extremely noisy labels. In *Advances in neural information processing systems*, pages 8527–8537.

HaoChen, J. Z., Wei, C., Lee, J., and Ma, T. (2021). Shape matters: Understanding the implicit bias of the noise covariance. In *Conference on Learning Theory*, pages 2315–2357. PMLR.

Hardt, M., Recht, B., and Singer, Y. (2016). Train faster, generalize better: Stability of stochastic gradient descent. In *International Conference on Machine Learning*, pages 1225–1234.

He, K., Zhang, X., Ren, S., and Sun, J. (2016). Deep residual learning for image recognition. In *Proceedings of the IEEE conference on computer vision and pattern recognition*, pages 770–778.

Hochreiter, S. and Schmidhuber, J. (1995). Simplifying neural nets by discovering flat minima. In *Advances in neural information processing systems*, pages 529–536.

Hochreiter, S. and Schmidhuber, J. (1997). Flat minima. *Neural Computation*, 9(1):1–42.

Hodgkinson, L. and Mahoney, M. (2021). Multiplicative noise and heavy tails in stochastic optimization. In *International Conference on Machine Learning*, pages 4262–4274. PMLR.

Jacot, A., Gabriel, F., and Hongler, C. (2019). The asymptotic spectrum of the hessian of dnn throughout training. In *International Conference on Learning Representations*.

Jastrzkebski, S., Kenton, Z., Arpit, D., Ballas, N., Fischer, A., Bengio, Y., and Storkey, A. (2017). Three factors influencing minima in sgd. *arXiv preprint arXiv:1711.04623*.

Kingma, D. P. and Ba, J. (2015). Adam: A method for stochastic optimization. *3rd International Conference on Learning Representations, ICLR 2015*.

Krizhevsky, A. and Hinton, G. (2009). Learning multiple layers of features from tiny images.

LeCun, Y. (1998). The mnist database of handwritten digits. *http://yann. lecun. com/exdb/mnist/*.

LeCun, Y., Bengio, Y., and Hinton, G. (2015). Deep learning. *nature*, 521(7553):436.

LeCun, Y., Bottou, L., Bengio, Y., and Haffner, P. (1998). Gradient-based learning applied to document recognition. *Proceedings of the IEEE*, 86(11):2278–2324.

Li, X., Gu, Q., Zhou, Y., Chen, T., and Banerjee, A. (2020). Hessian based analysis of sgd for deep nets: Dynamics and generalization. In *Proceedings of the 2020 SIAM International Conference on Data Mining*, pages 190–198. SIAM.

Li, Z., Malladi, S., and Arora, S. (2021a). On the validity of modeling SGD with stochastic differential equations (SDEs). In *Thirty-Fifth Conference on Neural Information Processing Systems*.

Li, Z., Malladi, S., and Arora, S. (2021b). On the validity of modeling sgd with stochastic differential equations (sdes). *arXiv preprint arXiv:2102.12470*.

Liao, Z. and Mahoney, M. W. (2021). Hessian eigenspectra of more realistic nonlinear models. *Advances in Neural Information Processing Systems*, 34.

Liu, K., Ziyin, L., and Ueda, M. (2021). Noise and fluctuation of finite learning rate stochastic gradient descent. In *International Conference on Machine Learning*, pages 7045–7056. PMLR.

Ma, Y., Yu, D., Wu, T., and Wang, H. (2019). Paddlepaddle: An open-source deep learning platform from industrial practice. *Frontiers of Data and Domputing*, 1(1):105–115.

Mandt, S., Hoffman, M. D., and Blei, D. M. (2017). Stochastic gradient descent as approximate bayesian inference. *The Journal of Machine Learning Research*, 18(1):4873–4907.

Martin, C. H. and Mahoney, M. W. (2017). Rethinking generalization requires revisiting old ideas: statistical mechanics approaches and complex learning behavior. *arXiv preprint arXiv:1710.09553*.

https://doi.org/10.52202/075280-2892

Massey Jr, F. J. (1951). The kolmogorov-smirnov test for goodness of fit. *Journal of the American statistical Association*, 46(253):68–78.

Myung, I. J. (2003). Tutorial on maximum likelihood estimation. *Journal of mathematical Psychology*, 47(1):90–100.

Panigrahi, A., Somani, R., Goyal, N., and Netrapalli, P. (2019). Non-gaussianity of stochastic gradient noise. *arXiv preprint arXiv:1910.09626*.

Papyan, V. (2018). The full spectrum of deepnet hessians at scale: Dynamics with sgd training and sample size. *arXiv preprint arXiv:1811.07062*.

Papyan, V. (2019). Measurements of three-level hierarchical structure in the outliers in the spectrum of deepnet hessians. In *International Conference on Machine Learning*, pages 5012–5021. PMLR.

Paszke, A., Gross, S., Massa, F., Lerer, A., Bradbury, J., Chanan, G., Killeen, T., Lin, Z., Gimelshein, N., Antiga, L., et al. (2019). Pytorch: An imperative style, high-performance deep learning library. In *Advances in neural information processing systems*, pages 8026–8037.

Pawitan, Y. (2001). *In all likelihood: statistical modelling and inference using likelihood*. Oxford University Press.

Pennington, J. and Bahri, Y. (2017). Geometry of neural network loss surfaces via random matrix theory. In *International Conference on Machine Learning*, pages 2798–2806. PMLR.

Pennington, J. and Worah, P. (2018). The spectrum of the fisher information matrix of a single-hidden-layer neural network. In *NeurIPS*, pages 5415–5424.

Plackett, R. L. (1983). Karl pearson and the chi-squared test. *International statistical review/revue internationale de statistique*, pages 59–72.

Reuveni, S., Granek, R., and Klafter, J. (2008). Proteins: coexistence of stability and flexibility. *Physical review letters*, 100(20):208101.

Sagun, L., Bottou, L., and LeCun, Y. (2016). Eigenvalues of the hessian in deep learning: Singularity and beyond. *arXiv preprint arXiv:1611.07476*.

Sagun, L., Evci, U., Guney, V. U., Dauphin, Y., and Bottou, L. (2017). Empirical analysis of the hessian of over-parametrized neural networks. *arXiv preprint arXiv:1706.04454*.

Sekhari, A., Sridharan, K., and Kale, S. (2021). Sgd: The role of implicit regularization, batch-size and multiple-epochs. *Advances in Neural Information Processing Systems*, 34.

Simsekli, U., Sagun, L., and Gurbuzbalaban, M. (2019). A tail-index analysis of stochastic gradient noise in deep neural networks. In *International Conference on Machine Learning*, pages 5827–5837.

Singh, S. P., Bachmann, G., and Hofmann, T. (2021). Analytic insights into structure and rank of neural network hessian maps. *Advances in Neural Information Processing Systems*, 34:23914–23927.

Smith, S. L., Dherin, B., Barrett, D., and De, S. (2020). On the origin of implicit regularization in stochastic gradient descent. In *International Conference on Learning Representations*.

Stringer, C., Pachitariu, M., Steinmetz, N., Carandini, M., and Harris, K. D. (2019). High-dimensional geometry of population responses in visual cortex. *Nature*, 571(7765):361–365.

Sutskever, I., Martens, J., Dahl, G., and Hinton, G. (2013). On the importance of initialization and momentum in deep learning. In *International conference on machine learning*.

Tang, Q.-Y. and Kaneko, K. (2020). Long-range correlation in protein dynamics: Confirmation by structural data and normal mode analysis. *PLoS computational biology*, 16(2):e1007670.

Torralba, A. and Oliva, A. (2003). Statistics of natural image categories. *Network: computation in neural systems*, 14(3):391.

https://doi.org/10.52202/075280-2892

Virtanen, P., Gommers, R., Oliphant, T. E., Haberland, M., Reddy, T., Cournapeau, D., Burovski, E., Peterson, P., Weckesser, W., Bright, J., et al. (2020). Scipy 1.0: fundamental algorithms for scientific computing in python. *Nature methods*, 17(3):261–272.

Visser, M. (2013). Zipf's law, power laws and maximum entropy. *New Journal of Physics*, 15(4):043021.

Wen, Y., Luk, K., Gazeau, M., Zhang, G., Chan, H., and Ba, J. (2020). An empirical study of stochastic gradient descent with structured covariance noise. In Chiappa, S. and Calandra, R., editors, *Proceedings of the Twenty Third International Conference on Artificial Intelligence and Statistics*, volume 108 of *Proceedings of Machine Learning Research*, pages 3621–3631. PMLR.

Wu, J., Hu, W., Xiong, H., Huan, J., Braverman, V., and Zhu, Z. (2020). On the noisy gradient descent that generalizes as sgd. In *International Conference on Machine Learning*, pages 10367–10376. PMLR.

Wu, J., Zou, D., Braverman, V., and Gu, Q. (2021). Direction matters: On the implicit regularization effect of stochastic gradient descent with moderate learning rate. *International Conference on Learning Representations*.

Wu, L., Zhu, Z., et al. (2017). Towards understanding generalization of deep learning: Perspective of loss landscapes. *arXiv preprint arXiv:1706.10239*.

Xie, Z., He, F., Fu, S., Sato, I., Tao, D., and Sugiyama, M. (2021a). Artificial neural variability for deep learning: On overfitting, noise memorization, and catastrophic forgetting. *Neural Computation*, 33(8).

Xie, Z., Sato, I., and Sugiyama, M. (2021b). A diffusion theory for deep learning dynamics: Stochastic gradient descent exponentially favors flat minima. In *International Conference on Learning Representations*.

Xie, Z., Tang, Q.-Y., Cai, Y., Sun, M., and Li, P. (2022a). On the power-law spectrum in deep learning: A bridge to protein science. *arXiv preprint arXiv:2201.13011*.

Xie, Z., Wang, X., Zhang, H., Sato, I., and Sugiyama, M. (2022b). Adaptive inertia: Disentangling the effects of adaptive learning rate and momentum. In *Proceedings of the 39th International Conference on Machine Learning*, volume 162 of *Proceedings of Machine Learning Research*, pages 24430–24459.

Xie, Z., Xu, Z., Zhang, J., Sato, I., and Sugiyama, M. (2023). On the overlooked pitfalls of weight decay and how to mitigate them: A gradient-norm perspective. In *Thirty-seventh Conference on Neural Information Processing Systems*.

Xie, Z., Yuan, L., Zhu, Z., and Sugiyama, M. (2021c). Positive-negative momentum: Manipulating stochastic gradient noise to improve generalization. In *International Conference on Machine Learning*, volume 139 of *Proceedings of Machine Learning Research*, pages 11448–11458. PMLR.

Yao, Z., Gholami, A., Lei, Q., Keutzer, K., and Mahoney, M. W. (2018). Hessian-based analysis of large batch training and robustness to adversaries. In *Advances in Neural Information Processing Systems*, pages 4949–4959.

Yu, Y., Wang, T., and Samworth, R. J. (2015). A useful variant of the davis–kahan theorem for statisticians. *Biometrika*, 102(2):315–323.

Zhang, J., He, T., Sra, S., and Jadbabaie, A. (2019). Why gradient clipping accelerates training: A theoretical justification for adaptivity. In *International Conference on Learning Representations*.

Zhao, P., Chen, P.-Y., Das, P., Ramamurthy, K. N., and Lin, X. (2019). Bridging mode connectivity in loss landscapes and adversarial robustness. In *International Conference on Learning Representations*.

Zhu, Z., Wu, J., Yu, B., Wu, L., and Ma, J. (2019). The anisotropic noise in stochastic gradient descent: Its behavior of escaping from sharp minima and regularization effects. In *ICML*, pages 7654–7663.

Ziyin, L., Liu, K., Mori, T., and Ueda, M. (2022). Strength of minibatch noise in SGD. In *International Conference on Learning Representations*.

https://doi.org/10.52202/075280-2892

A Experimental Settings

Computational environment. The experiments are conducted on a computing cluster with NVIDIA® V100 GPUs and Intel® Xeon® CPUs. We can produce/reproduce the main experiments using PaddlePaddle (Ma et al., 2019) and PyTorch (Paszke et al., 2019).

Model: LeNet (LeCun et al., 1998), Fully Connected Networks (FCN), and ResNet18 (He et al., 2016). **Dataset**: MNIST (LeCun, 1998), CIFAR-10/100 (Krizhevsky and Hinton, 2009), and Avila (De Stefano et al., 2018). Avila is a non-image dataset.

A.1 Gradient History Matrices

In this paper, we compute the Gradient History Matrices and the covariance for multiple models on multiple datasets. Then, we use the elements in Gradient History Matrices and the eigenvalues of the covariance/second-moment to evaluate the goodness of fitting Gaussian distributions or power-law distributions via χ^2 tests and KS tests.

The Gradient History Matrix is an $n \times T$ matrix. For the experiment of LeNet and FCN, we compute the gradients for $T = 5000$ iterations at a fixed randomly initialized position $\theta^{(0)}$ or a pretrained position $\theta^\star$. Due to limit of memory capacity, for the experiment of ResNet18, we compute the gradients for $T = 200$ iterations at $\theta^{(0)}$ or $\theta^\star$.

A Gradient History Matrix can be used to compute the covariance or the second moment of stochastic gradients for a neural network. Note that a covariance matrix is an $n \times n$ matrix, which is extremely large for modern neural networks. Thus, we mainly analyze the gradient structures of LeNet and FCN at an affordable computational cost.

A.2 Models and Datasets

Models: LeNet (LeCun et al., 1998), Fully Connected Networks (FCN), and ResNet18 (He et al., 2016). We mainly used two-layer FCN which has 70 neurons for each hidden layer, ReLu activations, and BatchNorm layers, unless we specify otherwise.

Datasets: MNIST (LeCun, 1998) and CIFAR-10/100 (Krizhevsky and Hinton, 2009), and non-image Avila (De Stefano et al., 2018).

Optimizers: SGD, SGD with Momentum, and Adam (Kingma and Ba, 2015).

A.3 Image classification on MNIST

We perform the common per-pixel zero-mean unit-variance normalization as data preprocessing for MNIST.

Pretraining Hyperparameter Settings: We train neural networks for 50 epochs on MNIST for obtaining pretrained models. For the learning rate schedule, the learning rate is divided by 10 at the epoch of 40% and 80%. We use $\eta = 0.1$ for SGD/Momentum and $\eta = 0.001$ for Adam. The batch size is set to 128. The strength of weight decay defaults to $\lambda = 0.0005$ for pretrained models. We set the momentum hyperparameter $\beta_1 = 0.9$ for SGD Momentum. As for other optimizer hyperparameters, we apply the default settings directly.

Hyperparameter Settings for G: We use $\eta = 0.1$ for SGD/Momentum and $\eta = 0.001$ for Adam. The batch size is set to 1 and no weight decay is used, unless we specify them otherwise.

A.4 Image classification on CIFAR-10 and CIFAR-100

Data Preprocessing For CIFAR-10 and CIFAR-100: We perform the common per-pixel zero-mean unit-variance normalization, horizontal random flip, and 32×32 random crops after padding with 4 pixels on each side.

Pretraining Hyperparameter Settings: In the experiments on CIFAR-10 and CIFAR-100: $\eta = 1$ for Vanilla SGD; $\eta = 0.1$ for SGD (with Momentum); $\eta = 0.001$ for Adam. For the learning rate schedule, the learning rate is divided by 10 at the epoch of $\{80, 160\}$ for CIFAR-10 and $\{100, 150\}$ for CIFAR-100, respectively. The batch size is set to 128 for both CIFAR-10 and CIFAR-100. The

https://doi.org/10.52202/075280-2892

batch size is set to 128 for MNIST, unless we specify it otherwise. The strength of weight decay defaults to $\lambda = 0.0005$ as the baseline for all optimizers unless we specify it otherwise. We set the momentum hyperparameter $\beta_1 = 0.9$ for SGD and adaptive gradient methods which involve in Momentum. As for other optimizer hyperparameters, we apply the default settings directly.

Hyperparameter Settings for G: We use $\eta = 1$ for SGD, $\eta = 0.1$ for SGD with Momentum, and $\eta = 0.001$ for Adam. The batch size is set to 1 and no weight decay is used, unless we specify them otherwise.

A.5 Learning with noisy labels

We trained LeNet via SGD (with Momentum) on corrupted MNIST with various (asymmetric) label noise. We followed the setting of Han et al. (2018) for generating noisy labels for MNIST. The symmetric label noise is generated by flipping every label to other labels with uniform flip rates $\{40\%, 80\%\}$. In this paper, we used symmetric label noise.

For obtaining datasets with random labels which have little knowledge behind the pairs of instances and labels, we also randomly shuffle the labels of MNIST to produce Random MNIST.

B Goodness-of-Fit Tests

B.1 Kolmogorov-Smirnov Test

In this section, we introduce how to conduct the Kolmogorov-Smirnov Goodness-of-Fit Test.

We used Maximum Likelihood Estimation (MLE) (Myung, 2003; Clauset et al., 2009) for estimating the parameter β of the fitted power-law distributions and the Kolmogorov-Smirnov Test (KS Test) (Massey Jr, 1951; Goldstein et al., 2004) for statistically testing the goodness of fitting power-law distributions. The KS test statistic is the KS distance d_{ks} between the hypothesized (fitted) distribution and the empirical data, which measures the goodness of fit. It is defined as

$$d_{\mathrm{ks}} = \sup_{\lambda} |F^{\star}(\lambda) - \hat{F}(\lambda)|, \tag{7}$$

where $F^{\star}(\lambda)$ is the hypothesized cumulative distribution function and $\hat{F}(\lambda)$ is the empirical cumulative distribution function based on the sampled data (Goldstein et al., 2004). The estimated power exponent via MLE (Clauset et al., 2009) can be written as

$$\hat{\beta} = 1 + K \left[\sum_{i=1}^{K} \ln \left(\frac{\lambda_i}{\lambda_{\min}} \right) \right]^{-1}, \tag{8}$$

where K is the number of tested samples and we set $\lambda_{\min} = \lambda_k$. In this paper, we choose the top $K = 1000$ data points for the power-law hypothesis tests, unless we specify it otherwise. We note that the Powerlaw library (Alstott et al., 2014) provides a convenient tool to compute the KS distance, d_{ks}, and estimate the power exponent.

According to the practice of Kolmogorov-Smirnov Test (Massey Jr, 1951), we state ***the null hypothesis*** that the tested spectrum is not power-law. We state the alternative hypothesis, called ***the power-law hypothesis***, that the tested spectrum is power-law. If d_{ks} is higher than the critical value d_{c} at the $\alpha = 0.05$ significance level, we would accept the null hypothesis. In contrast, if d_{ks} is lower than the critical value d_{c} at the $\alpha = 0.05$ significance level, we would reject the null hypothesis and accept the power-law hypothesis.

For each KS test in this paper, we select top $k = 1000$ data points from dimension-wise gradients and iteration-wise gradients and top $k = 1000$ covariance eigenvalues as the tested sets to measure the goodness of power laws. We choose the largest data points for two reasons. First, focusing on relatively large values is very reasonable and common in various fields' power-law studies (Stringer et al., 2019; Reuveni et al., 2008; Tang and Kaneko, 2020), as real-world distributions typically follow power laws only after/large than some cutoff values (Clauset et al., 2009) for ensuring the convergence of the probability distribution. Second, researchers are usually more interested in significantly large eigenvalues due to the low-rank matrix approximation.

https://doi.org/10.52202/075280-2892

B.2 χ^2 Test

In this section, we introduce how we conduct χ^2 Test to evaluate the Gaussianity.

We directly used the χ^2 Normal Test implemented by the classical Python-based scientific computing package, Scipy (Virtanen et al., 2020), to evaluate the Gaussianity of empirical data. Note that we need to normalize the empirical data via whitening (zero-mean and unit-variance) before the tests.

The Gaussianity test statistic, p-value, is returned by the squared sum of the statistics of Skewness Test and Kurtosis Test (Cain et al., 2017). Skewness is a measure of symmetry. A distribution or dataset is symmetric if it looks the same to the left and right of the center. Kurtosis is a measure of whether the data are heavy-tailed or light-tailed relative to a normal distribution. Empirical data with high kurtosis tend to have heavy tails. Empirical data with low kurtosis tend to have light tails. Thus, χ^2 Test can reflect both Gaussianity and heavy tails. In this paper, we randomly choose $K = 100$ data points for the Gaussian hypothesis tests, unless we specify it otherwise.

We may write the p-value return by χ^2 Test as

$$p = z_S^2 + z_K^2, \tag{9}$$

where z_S is the Skewness Test statistic and z_K is the Kurtosis Test statistic. There are a number of ways to compute z_S and z_K in practice. It is convenient to use the default two-sided setting in Virtanen et al. (2020). Please refer to Virtanen et al. (2020) and the source code of $stats.skewtest$ and $stats.kurtosistest$ for the detailed implementation.

For each χ^2 test in this paper, we randomly select $k = 100$ data points from both dimension-wise gradients and iteration-wise gradients as the tested set to measure the Gaussianity. The returned test statistic, p-value, is a classical indicator of the relative goodness of Gaussianity for two types of gradients.

C Statistical Test Results

We present the statistical test results of the eigengaps of the gradient covariances in Table 3 and the visualized results in Figure 16.

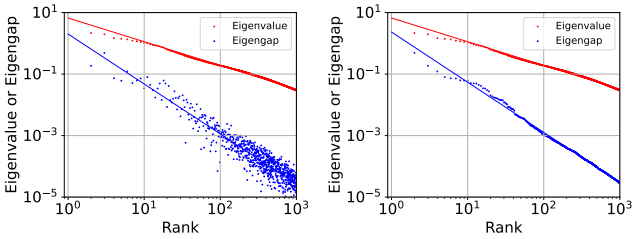

Figure 16: The eigengaps of stochastic gradient covariances are also approximately power-laws. Dataset: MNIST. Model: FCN. Left figure displays the eigengaps by original rank indices sorted by eigenvalues. Right figure displays the eigengaps by rank indices re-sorted by eigengaps.

Table 3: KS statistics of the covariance eigengaps of LeNet and FCN.

Dataset	Model	Training	d_{ks}	d_{c}	Power-Law	$\hat{s}$
MNIST	LeNet	Pretrain	0.0205	0.043	Yes	5.111
MNIST	LeNet	Random	0.0221	0.043	Yes	2.232
MNIST	FCN	Pretrain	0.0219	0.043	Yes	1.668
MNIST	FCN	Random	0.0231	0.043	Yes	1.668

We present the statistical test results of dimension-wise gradients and iteration-wise gradients of LeNet and ResNet18 on various datasets in Tables 4 and 5.

We conducted the KS Tests for all of our studied covariance spectra. We display the KS test statistics and the estimated power exponents $\hat{s}$ in the tables. For better visualization, we color accepting the power-law hypothesis in blue and color accepting the null hypothesis (and the cause) in red. The KS Test statistics of the covariance spectra are shown in Tables 6, 7, 8, 9, 10, and 11.

https://doi.org/10.52202/075280-2892

Table 4: The KS and χ^2 statistics and the hypothesis acceptance rates of iteration-wise gradients with respect to the batch size. Model: LeNet. Dataset: MNIST

Type	Training	Setting	$\bar{d}_{\text{ks}}$	d_{c}	Power-Law Rate	$\bar{p}$-value	Gaussian Rate
Iteration	Random	$B = 1$	0.428	0.0430	0.067%	0.047	12.6%
Iteration	Random	$B = 3$	0.385	0.0430	0.17%	0.089	21.5%
Iteration	Random	$B = 10$	0.267	0.0430	0.25%	0.173	28.5%
Iteration	Random	$B = 30$	0.249	0.0430	0.16%	0.240	50.9%
Iteration	Random	$B = 100$	0.191	0.0430	0.079%	0.321	65.1%
Iteration	Random	$B = 300$	0.119	0.0430	0.033%	0.382	74.5%
Iteration	Random	$B = 1000$	0.120	0.0430	0.041%	0.388	75.5%
Dimension	Random	$B = 1$	0.0306	0.0430	90.6%	4.51×10^{-5}	0%
Dimension	Random	$B = 3$	0.0358	0.0430	74.5%	9.07×10^{-5}	0.02%
Dimension	Random	$B = 10$	0.0392	0.0430	65.3%	1.78×10^{-4}	0%
Dimension	Random	$B = 30$	0.0379	0.0430	68.9%	2.29×10^{-4}	0.14%
Dimension	Random	$B = 100$	0.0355	0.0430	76.6%	4.11×10^{-4}	0.18%
Dimension	Random	$B = 300$	0.0269	0.0430	97.5%	1.21×10^{-3}	0.48%
Dimension	Random	$B = 1000$	0.0309	0.0430	90.6%	1.43×10^{-4}	0%

Table 5: The KS and χ^2 statistics and the hypothesis acceptance rates of the gradients over dimensions and iterations, respectively. Model: ResNet18. Batch Size: 100. In the second column "random" means randomly initialized models, while "pretrain" means pretrained models.

Dataset	Training	SG Type	$\bar{d}_{\text{ks}}$	d_{c}	Power-Law Rate	$\bar{p}$-value	Gaussian Rate
CIFAR-10	Random	Dimension	0.0924	0.0962	54.3%	1.73×10^{-2}	6.4%
CIFAR-10	Random	Iteration	0.141	0.0962	1.32%	0.495	93.4%
CIFAR-10	Pretrain	Dimension	0.0717	0.0962	82.6%	1.1×10^{-2}	3.2%
CIFAR-10	Pretrain	Iteration	0.140	0.0962	1.38%	0.497	93.5%
CIFAR-100	Random	Dimension	0.0631	0.0962	92.4%	8.55×10^{-3}	3%
CIFAR-100	Random	Iteration	0.141	0.0962	1.36%	0.496	93.2%
CIFAR-100	Pretrain	Dimension	0.0637	0.0962	88.5%	8.11×10^{-3}	3.4%
CIFAR-100	Pretrain	Iteration	0.140	0.0962	1.37%	0.496	93.1%

Table 6: The KS statistics of the second-moment spectra of dimension-wise gradients for LeNet on MNIST.

Dataset	Model	Training	Batch	Sample size	Setting	d_{ks}	d_{c}	Power-Law	$\hat{s}$
MNIST	LeNet	Pretrain	1	1000	-	0.0206	0.0430	Yes	1.302
MNIST	LeNet	Pretrain	10	1000	-	0.0244	0.0430	Yes	1.313
MNIST	LeNet	Pretrain	100	1000	-	0.0171	0.0430	Yes	1.390
MNIST	LeNet	Pretrain	1000	1000	-	0.0173	0.0430	Yes	1.314
MNIST	LeNet	Pretrain	10000	1000	-	0.0204	0.0430	Yes	1.290
MNIST	LeNet	Pretrain	60000	1000	-	0.106	0.0430	No	0.206
MNIST	LeNet	Random	1	1000	-	0.0220	0.0430	Yes	1.428
MNIST	LeNet	Random	10	1000	-	0.0223	0.0430	Yes	1.334
MNIST	LeNet	Random	100	1000	-	0.0228	0.0430	Yes	1.313
MNIST	LeNet	Random	1000	1000	-	0.0198	0.0430	Yes	1.423
MNIST	LeNet	Random	10000	1000	-	0.0213	0.0430	Yes	1.284
MNIST	LeNet	Random	60000	1000	-	0.203	0.0430	No	0.271

https://doi.org/10.52202/075280-2892

Table 7: The KS statistics of the covariance spectra of dimension-wise gradients for LeNet on MNIST.

Dataset	Model	Training	Batch	Sample size	Setting	d_{ks}	d_{c}	Power-Law	$\hat{s}$
MNIST	LeNet	Random	1	1000	-	0.0226	0.0430	Yes	1.425
MNIST	LeNet	Random	10	1000	-	0.0227	0.0430	Yes	1.331
MNIST	LeNet	Random	100	1000	-	0.0230	0.0430	Yes	1.311
MNIST	LeNet	Random	1000	1000	-	0.0200	0.0430	Yes	1.423
MNIST	LeNet	Random	10000	1000	-	0.0287	0.0430	Yes	1.320
MNIST	LeNet	Pretrain	1	1000	-	0.0206	0.0430	Yes	1.299
MNIST	LeNet	Pretrain	10	1000	-	0.0247	0.0430	Yes	1.310
MNIST	LeNet	Pretrain	100	1000	-	0.0171	0.0430	Yes	1.386
MNIST	LeNet	Pretrain	1000	1000	-	0.0174	0.0430	Yes	1.312
MNIST	LeNet	Pretrain	10000	1000	-	0.0223	0.0430	Yes	1.331
MNIST	LeNet	Pretrain	1	1000	Label Noise 40%	0.0289	0.0430	Yes	1.453
MNIST	LeNet	Pretrain	1	1000	Label Noise 80%	0.0138	0.0430	Yes	11.442
MNIST	LeNet	Pretrain	1	1000	Random Label	0.0129	0.0430	Yes	1.374
MNIST	LeNet	Pretrain	1	1000	GradClip=1	0.0226	0.0430	Yes	1.323
MNIST	LeNet	Pretrain	1	1000	GradClip=0.1	0.0261	0.0430	Yes	1.343

Table 8: The KS statistics of the second-moment spectra of dimension-wise gradients for FCN on MNIST.

Dataset	Model	Training	Batch	Sample size	Setting	d_{ks}	d_{c}	Power-Law	$\hat{s}$
MNIST	2Layer-FCN	Pretrain	10	1000	-	0.0415	0.0430	Yes	0.866
MNIST	2Layer-FCN	Random	10	1000	-	0.0418	0.0430	Yes	0.864
MNIST	2Layer-FCN	Random	10	1000	Noise	0.0427	0.0430	Yes	0.862
MNIST	2Layer-FCN	Pretrain	10	1000	Width=70	0.0415	0.0430	Yes	0.866
MNIST	2Layer-FCN	Pretrain	10	1000	Width=30	0.0425	0.0430	Yes	0.869
MNIST	2Layer-FCN	Pretrain	10	1000	Width=10	0.0486	0.0430	No	
MNIST	2Layer-FCN	Random	10	1000	Width=70	0.0418	0.0430	Yes	0.864
MNIST	2Layer-FCN	Random	10	1000	Width=30	0.0488	0.0430	No	
MNIST	2Layer-FCN	Random	10	1000	Width=10	0.0491	0.0430	No	
MNIST	1Layer-FCN	Random	10	1000	-	0.0384	0.0430	Yes	1.357
MNIST	1Layer-FCN	Pretrain	10	1000	-	0.0384	0.0430	Yes	1.355

Table 9: The KS statistics of the second-moment spectra of dimension-wise gradients for LNN on MNIST.

Dataset	Model	Training	Batch	Sample size	Setting	d_{ks}	d_{c}	Power-Law	$\hat{s}$
MNIST	4Layer-LNN	Pretrain	10	1000	-	0.0445	0.0430	No	1.629
MNIST	4Layer-LNN	Pretrain	10	1000	BatchNorm	0.0268	0.0430	Yes	0.955
MNIST	4Layer-LNN	Pretrain	10	1000	ReLU	0.0154	0.0430	Yes	1.074

Table 10: The KS statistics of the covariance spectra of dimension-wise gradients for LeNet on CIFAR-10.

Dataset	Model	Training	Batch	Sample size	Setting	d_{ks}	d_{c}	Power-Law	$\hat{s}$
CIFAR-10	LeNet	Pretrain	1	1000	-	0.0201	0.0430	Yes	1.257
CIFAR-10	LeNet	Random	1	1000	-	0.0214	0.0430	Yes	1.300
CIFAR-10	LeNet	Pretrain	1	1000	GradClip=0.1	0.0244	0.0430	Yes	1.348
CIFAR-10	LeNet	Random	100	1000	SGD	0.00818	0.0430	Yes	1.305
CIFAR-10	LeNet	Random	100	1000	Weight Decay	0.0107	0.0430	Yes	1.300
CIFAR-10	LeNet	Random	100	1000	Momentum	0.00806	0.0430	Yes	1.262
CIFAR-10	LeNet	Random	100	1000	Adam	0.0634	0.0430	No	

https://doi.org/10.52202/075280-2892

Table 11: The KS statistics of the covariance spectra of LeNet on CIFAR-100.

Dataset	Model	Training	Batch	Sample size	Setting	d_{ks}	d_{c}	Power-Law	$\hat{s}$
CIFAR-100	LeNet	Pretrain	1	1000	-	0.0287	0.0430	Yes	1.276
CIFAR-100	LeNet	Random	1	1000	-	0.0307	0.0430	Yes	1.229
CIFAR-100	LeNet	Pretrain	1	1000	-	0.0197	0.0430	Yes	1.076

https://doi.org/10.52202/075280-2892